

Article

# A Scintillating One-Dimensional Coordination Polymer Based on Cadmium(II), *N,N'*-(1,4-Phenylenedicarbonyl)diglycinate, and 2,2'-Bipyridine: Crystal Structure, Hirshfeld Surface Analysis, and Luminescence Lifetime Properties †

Niels-Patrick Pook 

Institute of Inorganic and Analytical Chemistry, Clausthal University of Technology, Paul-Ernst-Str. 4, D-38678 Clausthal-Zellerfeld, Germany; niels-patrick.pook@tu-clausthal.de; Tel.: +49-5323-72-2887

† This work is dedicated to Arnold Adam on the occasion of his 65th birthday.

**Abstract:** In recent years, several coordination polymers of different dimensions and metal–organic frameworks were tested and expected to be good candidates for closing the gap between organic and plastic scintillators on the one hand side and inorganic scintillators on the other hand side. In the present work, we report the synthesis and characterization of a novel one-dimensional scintillating coordination polymer based on cadmium(II), *N,N'*-(1,4-phenylenedicarbonyl)di-glycinate, and 2,2'-bipyridine. Crystals could be obtained from water–methanol solutions and the structure was determined by single-crystal diffraction. The coordination polymer exhibits scintillation under X-ray excitation and laser as well as UV-light induced photoluminescence with fast decay times. Photoluminescence and X-ray excited optical luminescence (XEOL) properties and decay times were performed using a two-dimensional photon counting streak camera system with a time resolution up to 20 ps. The non-covalent interactions and supramolecular assemblies as a potential multiplier of the scintillating effect were investigated with the aid of a Hirshfeld surface analysis. The quality and phase purity of the used crystals and pellets was clarified by powder diffraction and Rietveld refinement.

**Keywords:** crystal structure; scintillation; cadmium(II) complex; *N,N'*-(1,4-phenylenedicarbonyl)diglycine; 2,2'-bipyridine ligand; supramolecular interactions; Hirshfeld surface analysis; decay time; X-ray excited optical luminescence; photoluminescence; lifetime spectroscopy



**Citation:** Pook, N.-P. A Scintillating One-Dimensional Coordination Polymer Based on Cadmium(II), *N,N'*-(1,4-Phenylenedicarbonyl)diglycinate, and 2,2'-Bipyridine: Crystal Structure, Hirshfeld Surface Analysis, and Luminescence Lifetime Properties. *Solids* **2021**, *2*, 371–384. <https://doi.org/10.3390/solids2040023>

Academic Editor: Timothy J. Prior

Received: 6 September 2021

Accepted: 19 October 2021

Published: 13 November 2021

**Publisher's Note:** MDPI stays neutral with regard to jurisdictional claims in published maps and institutional affiliations.



**Copyright:** © 2021 by the author. Licensee MDPI, Basel, Switzerland. This article is an open access article distributed under the terms and conditions of the Creative Commons Attribution (CC BY) license (<https://creativecommons.org/licenses/by/4.0/>).

## 1. Introduction

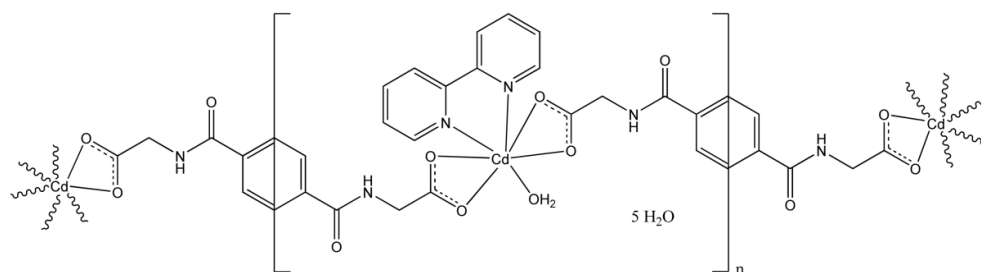
The discovery of X-rays in 1895 by Wilhelm Conrad Roentgen [1]—and thus the use of barium platino-cyanide and calcium tungstate [2] as fluorescent materials for the proof of X-rays—have paved the way of research and development on inorganic scintillation materials. Later, in the end of the 1940s, Kallman used naphthalene crystals for gamma-ray detection [3] (p. 531) and so the new class of organic scintillation materials was established.

Since this pioneering work, a lot of inorganic and organic scintillators (including plastic and liquid) have been synthesized and improved. Today, scintillators as materials for converting high-energy photons of X-rays, gamma-rays, and for highly-accelerated particles to visible or UV light photons are widely used for radiation detection in particle and high energy physics [4], in dosimetry of ionizing radiation and are very important for medical health care systems and diagnostics applications such as X-ray computed tomography imaging, single-photon emission computed tomography (SPECT) and positron emission tomography (PET) [5]. Furthermore, scintillating materials are the core elements of gamma-ray detection and X-ray imaging systems in borderline security. It is obvious that scintillators have a high importance for different areas of life and the search for further phosphors with these properties are more than relevant, especially since the possibility of

studying the spectral and time-resolved X-ray excited optical luminescence of materials with a table top device exists [6,7]. This presents a great opportunity in the search for new high energy transforming materials.

In addition to inorganic [8] and organic scintillators, the synthesis and structural investigation of metal–organic coordination polymers (CP) of different dimensions including metal–organic frameworks (MOFs) [9–12] have attracted much attention and gained a wide field in material science because of their functional architectures and potential applications in catalysis, gas storage [13], luminescence [14], and recently as scintillators [15–20]. The metal–organic CP based scintillators could be promising materials in complementing and in filling the gap between inorganic and organic scintillators and simultaneously founding a new area of high energy detection [17]. A major advantage of the combination of metals as connectors and organic ligands as linkers, with its many possible variations, is the large number of construction possibilities in creating scintillation materials designed for its specific range of application. Herein, a wise choice is the use of heavy metals with a high  $Z$  for an effective X-ray absorption process and the related generation of fast electrons, electron–hole pairs (excitons), and scattered radiation with lower energies which stimulate the aromatic ligands [21]. The emitted luminescence of the ligands can be detected in the spectral range of UV and visible light. The scintillation effect of most MOFs or CPs is based on the luminescence of the aromatic ligands. Very recently, a remarkable X-ray excited luminescence (XEL) of a lanthanides based metal–organic framework has been observed [19]. The tunable emitted wavelength (red to green) results from the metal centers and depends on the molar ratio of  $\text{Eu}^{3+}$  and  $\text{Tb}^{3+}$  in the MOF, but the phenanthroline ligand also plays an important role in receiving XEL.

However, it is known from the literature that electron-deficiency aromatic ring systems such as phenanthroline and bipyridine preferentially interact with  $\pi$ - $\pi$ -stacking interactions [22,23]. Therefore, the synthetic approach is to block several parts of a metal coordination environment with mentioned bidentate aromatic ligands and a simultaneously increasing of the  $\pi$ - $\pi$ -stacking interactions in the designed CP. In previously published works, during the search for new CP based scintillators, the coordination behavior of the  $N,N'$ -(1,4-phenylenedicarbonyl)diglycine in combination with mentioned electron-deficiency aromatic ligands and different first-row d-block metals or its complexes has been investigated and described in detail [24–27]. In the present work, a novel scintillating coordination polymer based on Cadmium(II), a metal center bridging and doubly bidentate  $N,N'$ -(1,4-phenylenedicarbonyl)diglycinate and bidentate bipyridine ligand has been synthesized (Scheme 1). The CP exhibits one-dimensional (1D) zigzag chains, which are linked over different non-covalent interactions. These weak interactions give raise to a three-dimensional (3D) supramolecular network.



**Scheme 1.** Schematic representation of the one-dimensional Cd(II) coordination polymer with 2,2'-bipyridine ligands, the metal-bridging  $N,N'$ -(1,4-phenylenedicarbonyl)diglycinate, and water molecules  $\{[\text{Cd}(\text{C}_{12}\text{H}_{10}\text{N}_2\text{O}_6)(\text{C}_{12}\text{H}_8\text{N}_2)(\text{H}_2\text{O})] \cdot 5\text{H}_2\text{O}\}_n$ .

## 2. Results

### 2.1. Description of the Crystal Structure

Colorless crystals of the CP were obtained from reactions of cadmium(II) nitrate, 2,2'-bipyridine, and  $N,N'$ -(1,4-phenylenedicarbonyl)diglycine in alkaline aqueous-methanol

solutions. The single-crystal X-ray structure analysis reveals that the formed 1D coordination polymer crystallizes in the centrosymmetric triclinic space group  $P\bar{1}$  (No. 2). The parameters of the single-crystal determination are listed in Table 1.

**Table 1.** Crystal data and structural refinement parameters of the cadmium(II) complex.

Compound	$\{[\text{Cd}(\text{C}_{12}\text{H}_{10}\text{N}_2\text{O}_6)(\text{C}_{12}\text{H}_8\text{N}_2)(\text{H}_2\text{O})] \cdot 5\text{H}_2\text{O}\}_n$
Empirical formula	$\text{C}_{22}\text{H}_{30}\text{CdN}_4\text{O}_{12}$
Formula weight	654.90
Temperature (K)	223
Diffractometer	Stoe IPDS II
Wavelength (Å)	0.71073
Crystal system	triclinic
Color	colorless
Space group	$P\bar{1}$ (No. 2)
$a, b, c$ (Å)	10.329(3), 11.424(2), 14.067(3)
$\alpha, \beta, \gamma$ (°)	98.266(17), 106.557(19), 115.422(18)
$V$ (Å <sup>3</sup> )	1367.5(6)
$Z$	2
$D_{\text{calc}}$ (g·cm <sup>−3</sup> )	1.591
$\mu$ (mm <sup>−1</sup> )	0.866
$F(000)$	668.0
Crystal size (mm)	0.500, 0.367, 0.150
$\theta$ Range (°)	2.190–26.499
	$-12 \leq h \leq 12$
Index ranges	$-12 \leq k \leq 14$
	$-17 \leq l \leq 17$
Reflection collected/unique	18,035/5647
Completeness to $\theta$ (%)	0.998
Absorption correction	Numerical; X-AREA, X-RED (2008)
Max. and min. transmission	0.7177/0.9016
Refinement method	Full-matrix least-squares on $F^2$
Data/parameters/restrains	5647/394/11
Goodness-of-Fit on $F^2$	1.054
$R_1 [I \geq 2\sigma(I)]/R_1$ (all data)	0.0358/0.0481
$wR_2 [I \geq 2\sigma(I)]/wR_2$ (all data)	0.0766/0.0807
Largest diff. peak and hole (e·Å <sup>−3</sup> )	0.986/−0.578
Deposition number	2062505

As shown in Figure 1, the repeated molecular unit of the zigzag chains consists of a Cd(II) metal center, two half  $N,N'$ -(1,4-phenylenedicarbonyl)diglycinate ligands, one coordinating water molecule and five solvent water molecules which are involved in classical and non-classical hydrogen bonding. The distorted seven-fold coordination of the Cd(II) center is constructed by four nitrogen atoms of the bidentate-chelating 2,2'-bipyridine, four oxygen atoms of two half bidentate  $N,N'$ -(1,4-phenylene-dicarbonyl)diglycinate ligands and one oxygen atom of a coordinating water molecule and shows a pentagonal-bipyramidal configuration. Two crystallographic centers of inversion are located at the centroids of the doubly-bidentate and metal centers bridging  $N,N'$ -(1,4-phenylenedicarbonyl)diglycinate ligands. The Cd–O distances ranges from 2.298 (5) to 2.574 (2) Å and the Cd–N distances are 2.328 (3) and 2.344 (3) Å. Distances and angles are in the expected ranges and comparable to those found in the literature [28–32]. Selected interatomic distances and angles are given in Table 2.

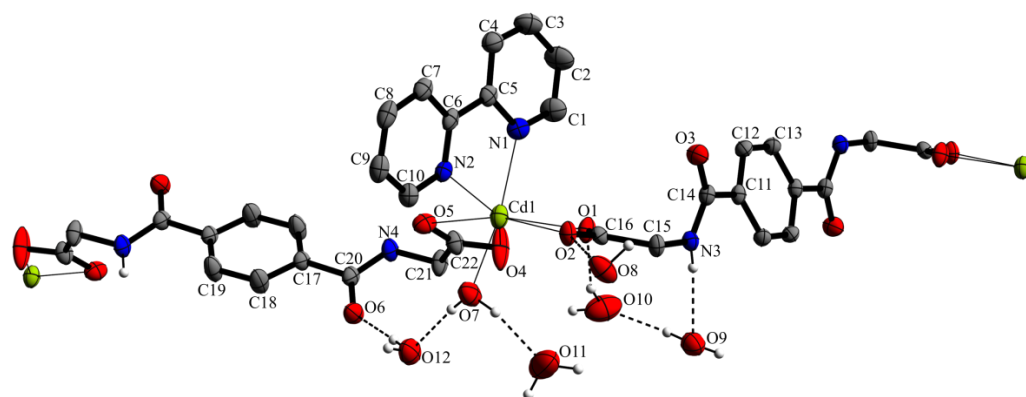


**Figure 1.** Molecular entities of the cadmium(II) coordination compound with atom labels and displacement ellipsoids of non-H atoms drawn at the 40% probability level. C–H···O, N–H···O, and O–H···O hydrogen bonds are shown as black dashed lines. The hydrogen atoms not involved in interactions have been omitted for clarity. Unlabeled atoms are related to labeled ones by the symmetry operation  $-x - 1, -y + 1, -z + 1$ , and  $-x + 1, -y + 1, -z$  (see Table 2 for details).

**Table 2.** Selected bond lengths (Å) and bond angle (°).

Bond	Lengths	Bond	Lengths
Cd1–O1	2.345 (2)	Cd1–O7	2.298 (3)
Cd1–O2	2.542 (2)	Cd1–N1	2.344 (3)
Cd1–O4	2.298 (5)	Cd1–N2	2.328 (3)
Cd1–O5	2.574 (2)		
Bond	Angle	Bond	Angle
N1–Cd1–N2	70.31 (10)	O1–Cd1–O2	53.43 (7)
N1–Cd1–O1	86.10 (9)	O1–Cd1–O4	78.04 (8)
N1–Cd1–O2	92.55 (9)	O1–Cd1–O5	130.21 (8)
N1–Cd1–O4	108.19 (14)	O1–Cd1–O7	104.59 (10)
N1–Cd1–O5	102.02 (9)	O2–Cd1–O4	125.80 (9)
N1–Cd1–O7	158.77 (10)	O2–Cd1–O5	165.04 (8)
N2–Cd1–O1	140.11 (8)	O2–Cd1–O7	79.93 (9)
N2–Cd1–O2	94.81 (8)	O4–Cd1–O5	52.57 (9)
N2–Cd1–O4	139.11 (9)	O4–Cd1–O7	92.13 (14)
N2–Cd1–O5	87.06 (8)	O5–Cd1–O7	85.22 (9)
N2–Cd1–O7	90.41 (11)		

The bond lengths of the carboxylate group of the  $N,N'$ -(1,4-phenylenedicarbonyl)-diglycinate ligands [C16–O1 = 1.254 (4) and C16–O2 = 1.256 (5) Å] as well as [C12–O4 = 1.249 (7) and C22–O2 = 1.226 (6) Å] indicate a delocalized bonding arrangement and are within the range of values found in previously described structures containing the  $N,N'$ -(1,4-phenylenedicarbonyl)diglycinate as ligand and as solvent molecule [24,25].

The nearly identical bond angles of the carboxylate groups O1–C16–O2 with 122.7 (5)° and O4–C22–O5 with 122.8 (3)° are decreased in comparison to the structures of the above-mentioned literature.

In the crystal structure, the supramolecular assembly is composed of different noncovalent interactions. In addition to the classical and non-classical hydrogen bonding of the carboxylates as well as the amide groups of the  $N,N'$ -(1,4-phenylenedicarbonyl)diglycinate ligands and water molecules, respectively, different  $\pi$ -stacking interactions are recognized (Figure 2). The hydrogen-bond geometries are in the expected ranges and summarized in Table S1 in the Supplementary Information file (SI).

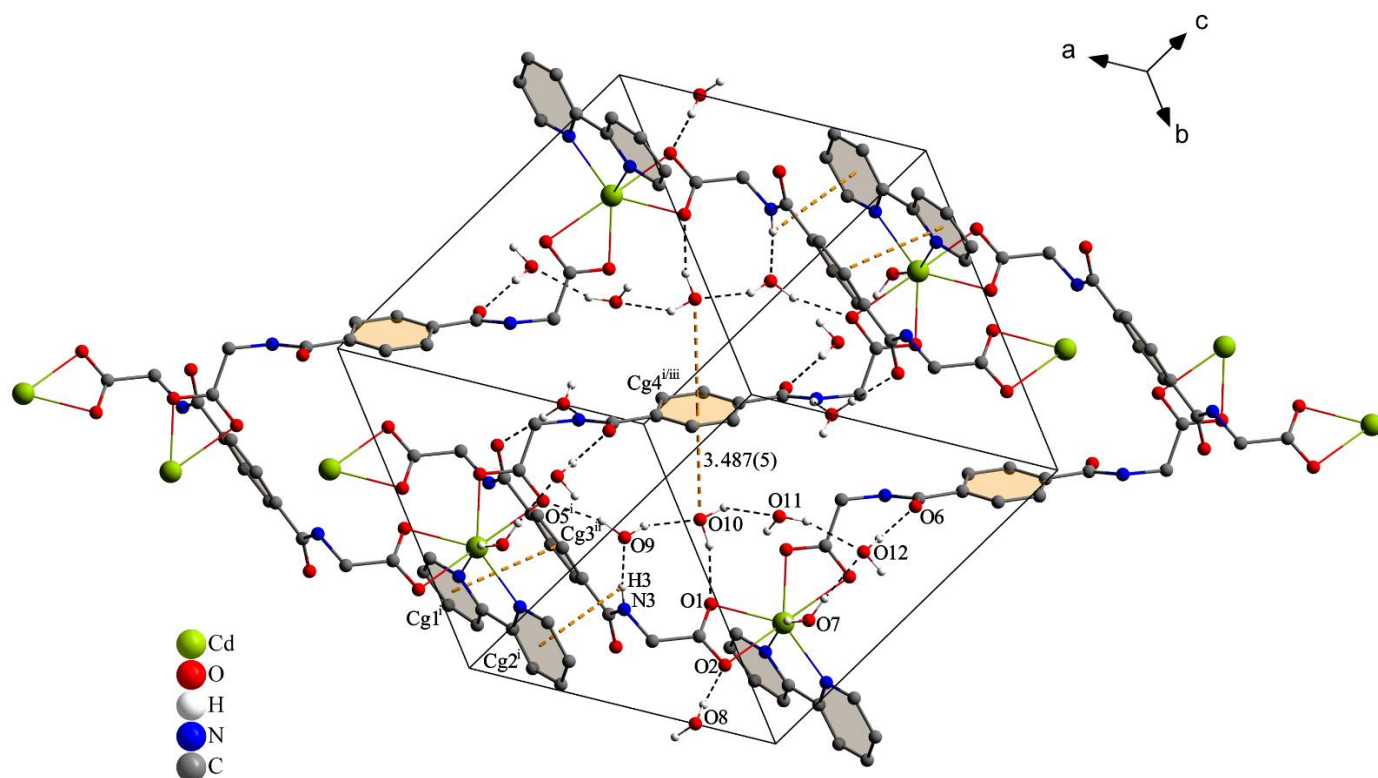


**Figure 2.** Perspective view of the unit cell of  $\{[\text{Cd}(\text{C}_{12}\text{H}_{10}\text{N}_2\text{O}_6)(\text{C}_{12}\text{H}_8\text{N}_2)(\text{H}_2\text{O})] \cdot 5\text{H}_2\text{O}\}_n$  with selected hydrogen bonds (black dashed lines) and lone-pair- $\pi$  and  $\pi$ - $\pi$  interactions (yellow dashed lines). The hydrogen atoms not involved in interactions have been omitted for clarity. Symmetry operations: (i)  $x + 1, y, z$ ; (ii)  $-x + 1, -y + 1, -z$ ; (iii)  $-x, -y + 1, -z + 1$ .

The bipyridine molecules are involved in  $\pi$ - $\pi$ -stacking and have an offset face-to-face arrangement, as depicted in Figures 2 and 3. The centroid-to-centroid distance is 3.765 (1) Å between Cg1...Cg2 where Cg1 and Cg2 are the centroids defined by ring atoms N1/C1–C5/C5 and N2/C6–C10, respectively. The  $N,N'$ -(1,4-phenylenedicarbonyl)diglycinate ligand L1 with the centroid Cg3 defined by the ring atoms C11–C13/C13'–C11' were stacked over  $\pi$ - $\pi$ -interactions with the bipyridine moiety Cg1 with a distance of 3.811 (1) Å. The short distance of N3–H3...Cg2 of the amide group of ligand L1 and the pyridine synthon Cg2 with 3.44 (1) Å is attributed to the N–H... $\pi$ -interaction (Figure 3). Comparable values for this stacking motif can be found in the literature [33,34]. The  $N,N'$ -(1,4-phenylenedicarbonyl)diglycinate ligand L2 with the centroid Cg4 defined by the ring atoms C17–C19/C17'–C19' is involved in lone-pair... $\pi$  interactions with the water molecule (O10) showing a distance of 3.487 (5) Å and an absence of  $\pi$ - $\pi$  stacking of the ligand L2 is observed (Figure 2). Similar values of these supramolecular interactions are described in the literature [35]. Against the background of a lately published CSD study, the directionality of the lone-pair... $\pi$  interactions can be discussed [36]. As a consequence, the 1D zigzag chains of the CP are linked through noncovalent interactions of classical and non-classical hydrogen bonding,  $\pi$ - $\pi$  stacking, N–H... $\pi$ - as well as lone-pair... $\pi$  interactions. These interactions compose a 3D supramolecular network.

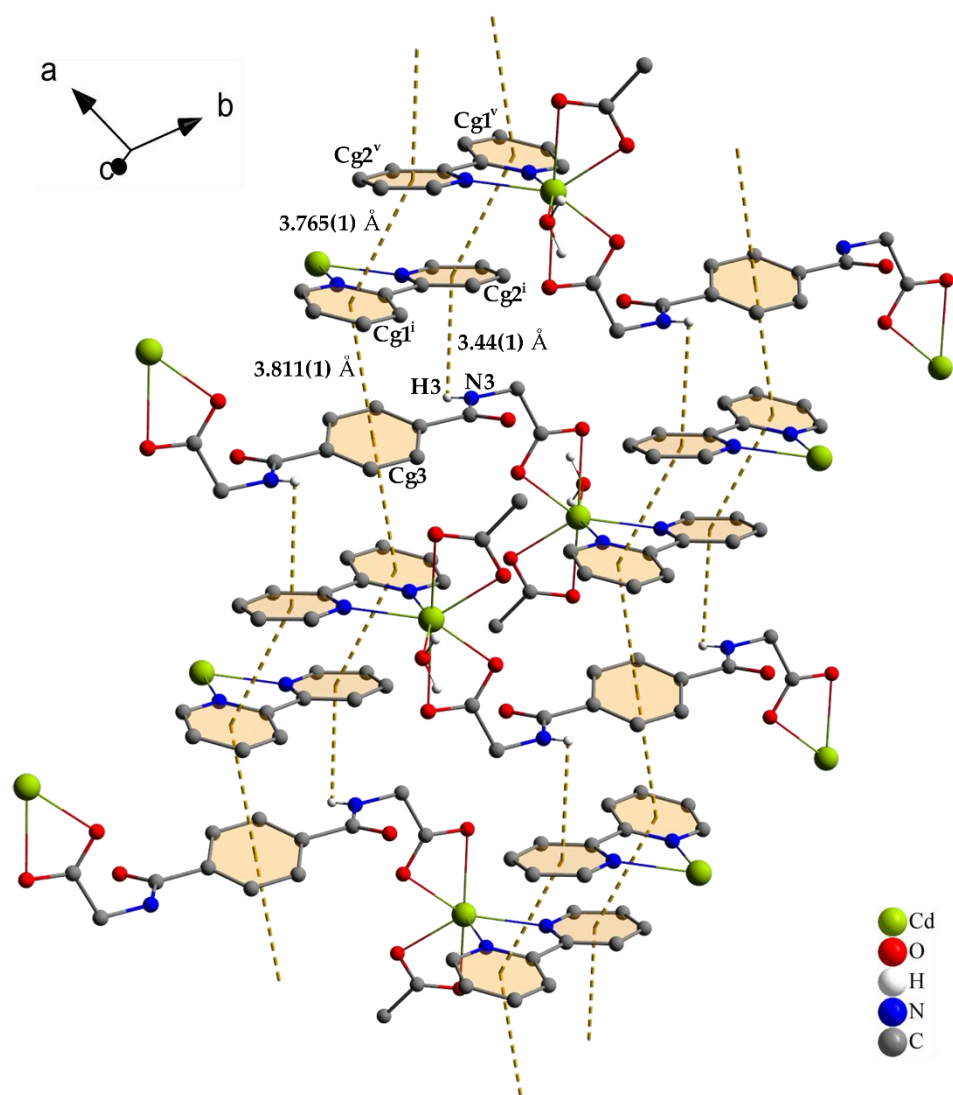


**Figure 3.** View of the 1D zigzag chain connections through  $\pi$ - $\pi$ - and N-H $\cdots$  $\pi$ -stacking interactions of the  $N,N'$ -(1,4-phenylenedicarbonyl)diglycinate ligand L2 and bipyridine ligands as well as bipyridine ligands of the supramolecular assembly. The hydrogen atoms not involved in interactions have been omitted for clarity. Symmetry codes: (i)  $x + 1, y, z$ ; (v)  $-x + 1, -y + 2, -z$ .

## 2.2. Hirshfeld Surface Analysis

The supramolecular assembly of the present crystal structure is mainly constructed by the noncovalent interactions of the metal coordinating ligands and water molecules. In order to quantify and explore these interactions, the different Hirshfeld surfaces (HS) are generated and visualized with the aid of CrystalExplorer [37] using TONTO with standard settings of the STO-3G basis set at Hartree–Fock theory. All calculated surfaces are drawn transparently to allow the view of all atoms and molecules around which the surface is calculated (Figure 4). The bright red spots of  $d_{\text{norm}}$  and the marked spikes and regions of the associated two-dimensional fingerprint plots indicate the classical and non-classical hydrogen bonding. Corresponding to the crystal structure description, the carboxylate and amide groups of the  $N,N'$ -(1,4-phenylenedicarbonyl)diglycinate ligands L1 and L2, as well as the C–H groups of the aromatic ligands are involved in these interactions.

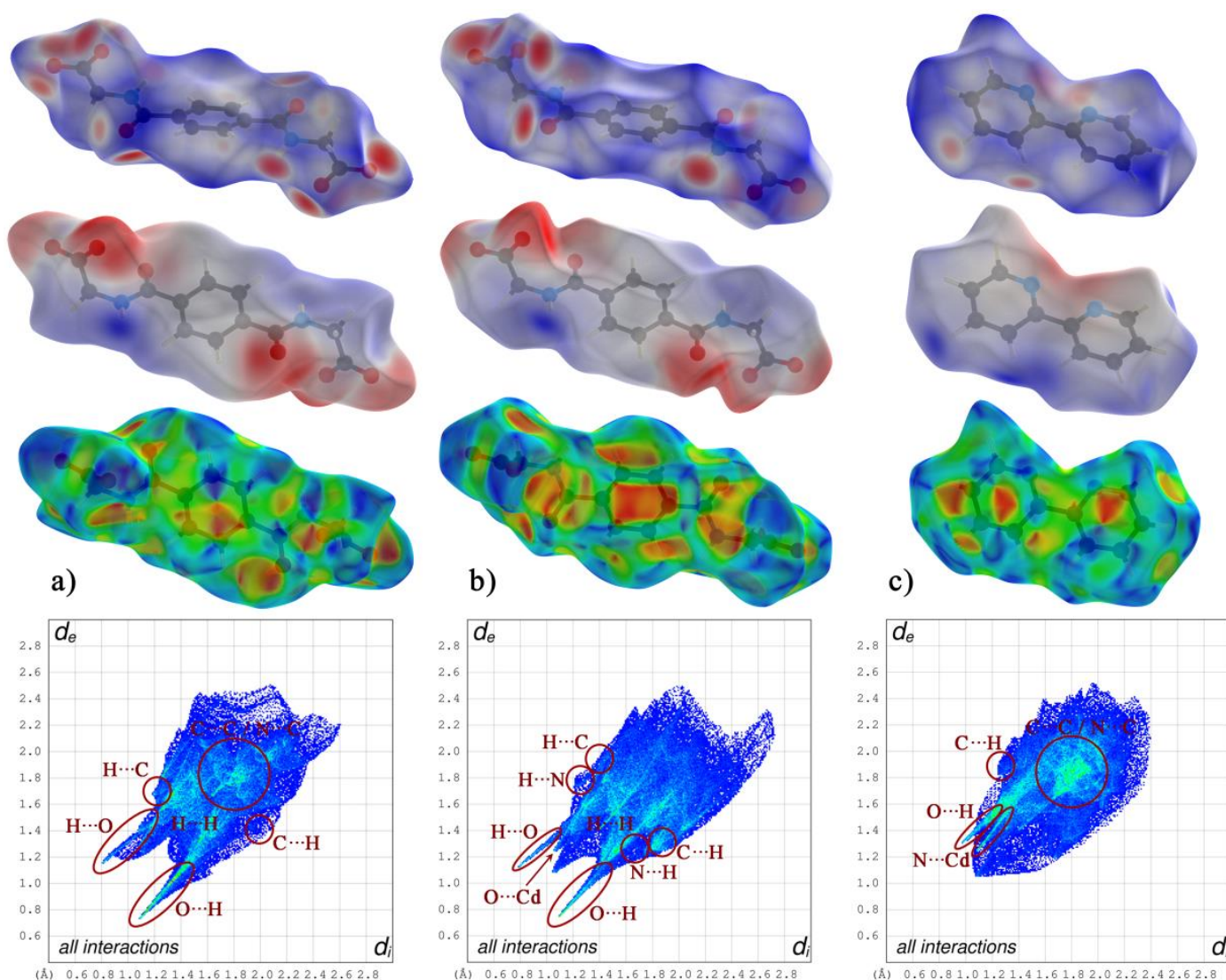


**Figure 4.** Hirshfeld surface analysis of ligands of the cadmium(II) coordination polymer. The two-dimensional fingerprint plots of all interactions, the graphical representations of the Hirshfeld surfaces mapped over the shape-index, the electrostatic potential energy and  $d_{\text{norm}}$  (from bottom to top) of (a) the  $N,N'$ -(1,4-phenylenedicarbonyl)diglycinate ligand L1, (b) the  $N,N'$ -(1,4-phenylenedicarbonyl)diglycinate ligand L2, and (c) 2,2'-bipyridine.

The HS mapped over the electrostatic potential energy reveals the donor and acceptor aspects of the mentioned groups. The blue areas indicate the positive and the red areas the negative electrostatic potential, respectively, and suggest that the oxygen atoms of the carboxylate and amide groups act as hydrogen-bond acceptors; whereas the nitrogen/hydrogen atoms of the amide groups and the carbon/hydrogen atoms of the aromatic moieties act as hydrogen-bond donors. The appearance of red and blue triangles of the HS mapped over the shape-index of the ligand (a) L1 and the (c) 2,2'-bipyridine represent the offset face-to-face  $\pi$ - $\pi$  stacking interaction as displayed in Figures 2 and 3. The lack of red and blue triangles and the occurrence of a large red region over the aromatic moiety of the ligand (b) L2 of the HS mapped over the shape-index exhibit the absence of a  $\pi$ - $\pi$  stacking motif and represent the deformation of the surface induced by a lone-pair. This observation corresponds to the lone-pair $\cdots\pi$  interaction of the water molecule (O10) with ligand L2 mentioned in the crystal structure description. A graphical representation of the different close contacts and their percentage contributions to the total HS of the ligands L1 as well as L2 and the 2,2'-bipyridine can be found in the Supplementary Information file (SI) as Figure S1.

### 2.3. X-ray Excited Optical Luminescence (XEOL) and Fluorescence Properties

The scintillation effect induced by X-rays is also known as X-ray excited luminescence (XEL) [19] or as X-ray excited optical luminescence (XEOL) [38]. The X-ray excited optical luminescence properties and decay times were performed using a two-dimensional photon counting streak camera system with a time resolution up to 20 ps. For further details of the instrumental set-up and sample preparation see Sections 3.4 and 3.4.1. The luminescence properties of the metal–organic CP have been investigated in the solid state and under ambient air conditions and room temperature. The material exhibits a significant fast scintillation under X-ray excitation with a decay time of 270 ps in the spectral range of 300 to 430 nm with an emission maximum at 363 nm (Figure 5). The accumulation time takes 21 h at a repetition rate of 10 MHz with a timing window of 10 ns and yielding in 104,458 counted photons. In most cases, scintillation materials can also be excited with UV light.

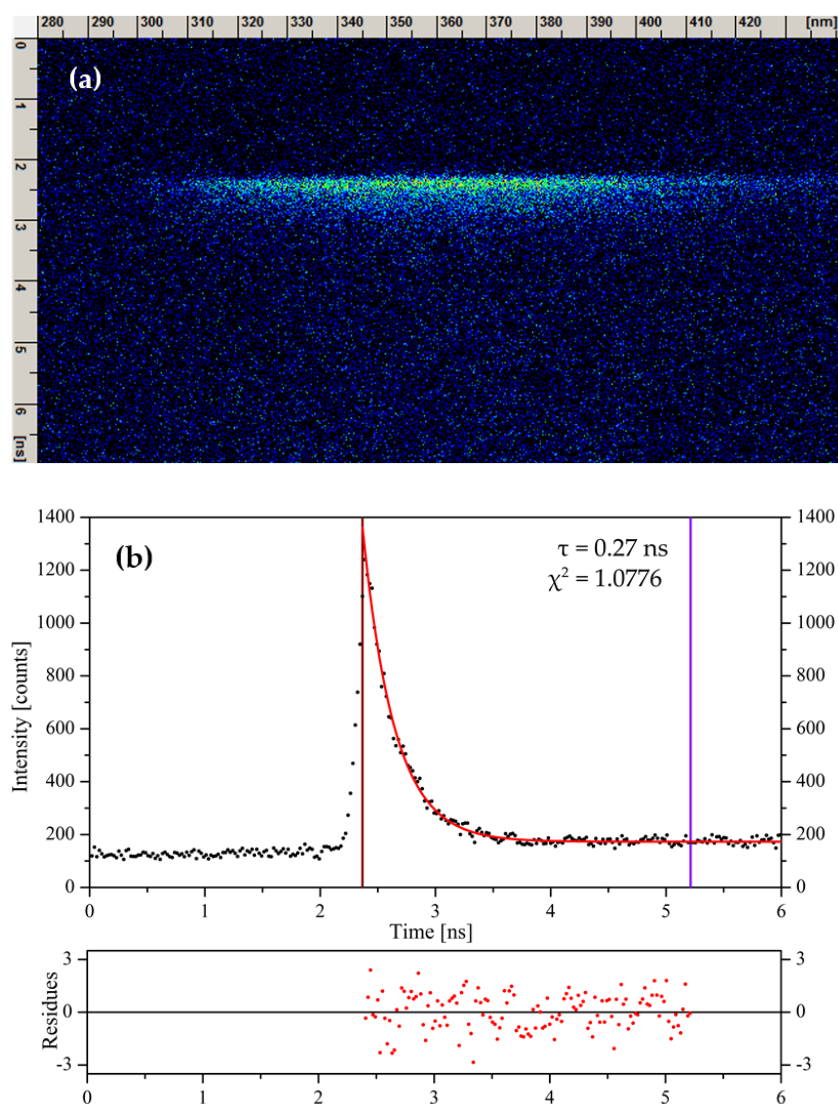


**Figure 5.** (a) Time-resolved streak image of X-ray (photon energy  $\sim 13\text{--}14$  keV,  $\sim 80$  ps pulse width) excited luminescence of the Cd(II) coordination polymer with corresponding (b) decay time fit and an accumulation time of 21 h at a repetition rate at 10 MHz.

Thus, the UV light (250 nm) induced fluorescence shows an emission in the spectral range of 300 to 450 nm with an emission maximum at 348 nm (Supplementary Information file, Figures S3 and S4). The emission maximum of the UV light induced fluorescence is a

little bit blue-shifted compared to the XEOL. The timing resolution is limited by the used pulsed UV-LED with a pulse width of 900 ps. For this reason, the fluorescence is too fast for accurate decay time fitting. An accumulation time of 180 min at a repetition rate of 10 MHz and a timing window of 20 ns have been chosen and yielded in 358,303 counted photons. The time-resolved streak image and measuring results of laser excited fluorescence are given in Figure 6. A measuring set-up with a timing window of 50 ns and an accumulation time of 2.5 h at a repetition rate of 10 MHz has been chosen.

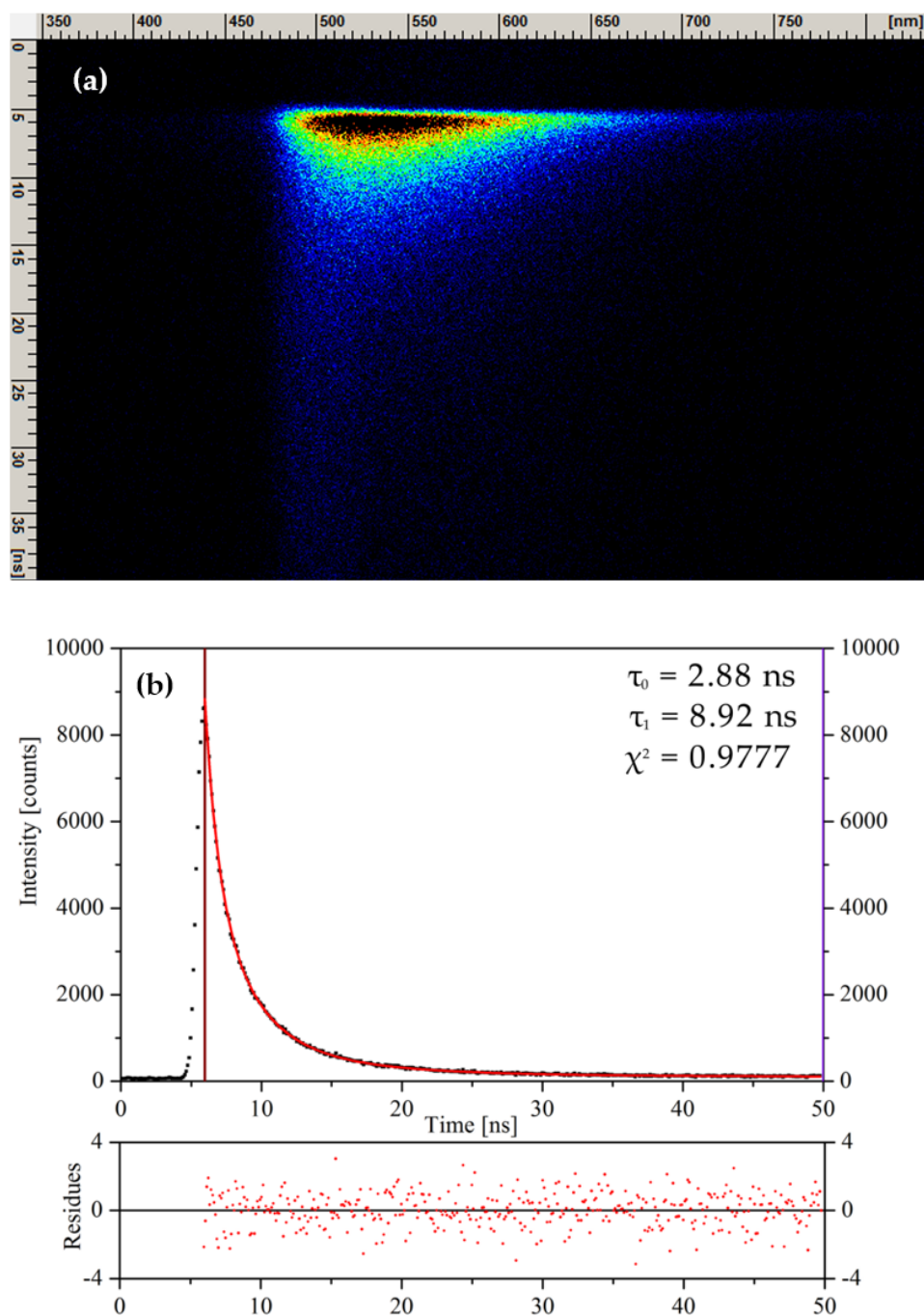


**Figure 6.** (a) Time-resolved streak image of laser ( $\lambda_{\text{ex}} = 444$  nm, 205 mW, 58 ps pulse width) induced fluorescence of the Cd(II) coordination polymer with corresponding (b) decay time fit and an accumulation time of 2.5 h at a repetition rate of 10 MHz.

A strong emission ( $\lambda_{\text{ex}} = 444$  nm) was observed in the spectral range of 460 to 750 nm with an emission maximum of 522 nm. During the measuring, a total number 330,661 pho-

tons have been counted. The corresponding spectra of all measurements can be found in the Supplementary Information file as Figures S2, S4, and S5.

Due to the fast emission under X-ray excitation, it is conceivable that the Cd(II) coordination polymer can be used for imaging applications such as PET systems, where a fast response of the scintillation material is essential for the accurate timing process of the detection system. Compared with other common scintillators, the novel coordination compound exhibits a fast emission but a relatively low light yield, even compared to well-known inorganic and organic scintillators measured with the used fluorescence lifetime spectroscopy system [6,7]. For this reason, future work will focus on the behavior under gamma-ray excitation, the investigation of the radiation hardness as well as the growth of larger crystals which are expected to give a higher light yield under the same measuring conditions.

#### 2.4. Rietveld Refinement

The phase purity of the used crystalline powder samples of the coordination compound were confirmed by powder diffraction techniques (more details see Section 3.3.) and Rietveld refinement using JANA2006 [39] program package. Figure 7 shows the summarized results of the Rietveld refinement. During the refinement procedure the single-crystal X-ray structure information of the CIF-file was loaded and compared with the measured powder pattern.

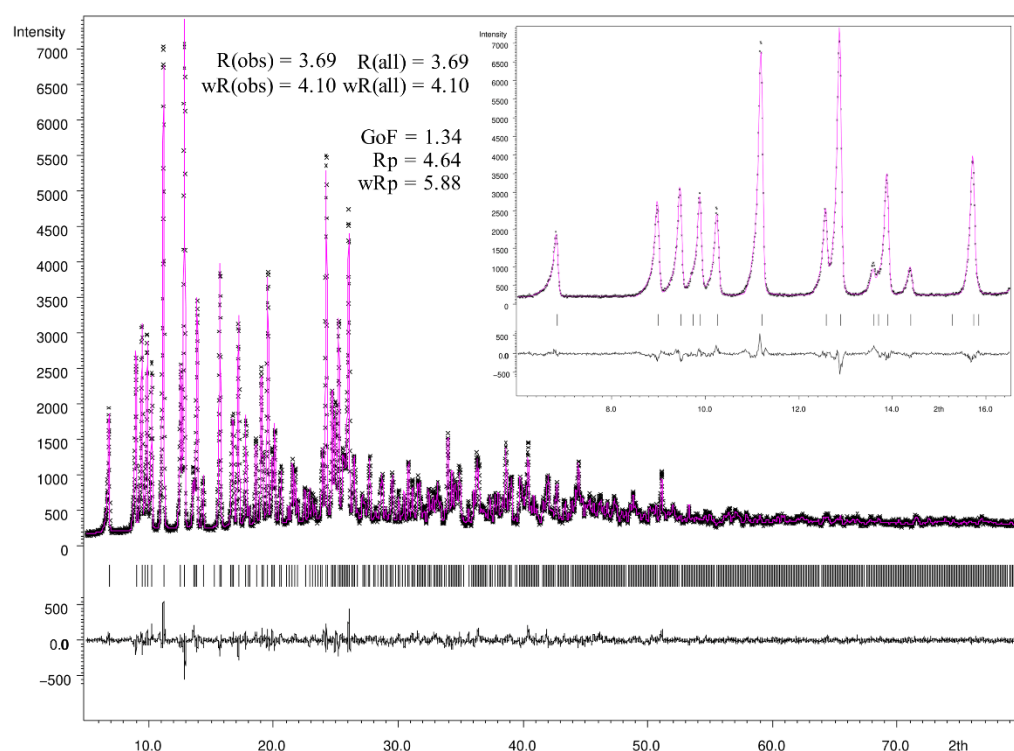


**Figure 7.** Observed (black crosses) and calculated (magenta line) X-ray powder diffraction pattern with difference profile of the Rietveld refinement (black line) as well as the positions of Bragg reflections (black bars) of a powder sample of the cadmium(II) coordination polymer.

During the Le Bail refinement and the profile matching procedure the parameters of the scale factor, background, unit cell parameters as well as peak shape, width, and peak symmetry were refined. The line shape of the diffraction peaks was described with the aid of the pseudo-Voigt function and the asymmetry of the low theta peaks were corrected by divergence, as depicted in Figure 7. In the following Rietveld refinement, all mentioned parameters were refined. The atomic distances ( $\pm 0.001$ ) and angles ( $\pm 0.01$ ) were weakly restrained while the ADPs were fixed to the ones of the single-crystal structure refinement.

Judged by the denoted quality factors and the figure of merit the results of the Rietveld refinement are well matched with the single-crystal structure determination.

### 3. Materials and Methods

#### 3.1. Syntheses of the Compound

Cesium carbonate (2 mmol), 2,2'-bipyridine (1 mmol), and *N,N'*-(1,4-phenylenediacarbonyl)diglycine (1 mmol) were dissolved in a 1:1 (*v/v*) mixture of water and methanol (50 mL). The mixture was heated and stirred for 1 h. After dissolving and cooling to room temperature, 10 mL of an aqueous solution of cadmium(II) nitrate (1 mmol) was slowly added under continuous stirring. Good quality colorless block-shaped crystals of the coordination polymer suitable for X-ray crystallography could be obtained after 2 days by slow evaporation under ambient conditions.

#### 3.2. Single-Crystal X-ray Crystallography

A well-shaped single-crystal of the cadmium(II) coordination compound with suitable dimensions was selected under a polarization microscope. It was carefully separated from the mother liquor with the aid of perfluorinated oil and finally placed in a glass fiber. The intensity data sets were collected on a Stoe IPDS II diffractometer using a graphite monochromated MoK $\alpha$  radiation ( $\lambda = 0.71073 \text{ \AA}$ ). The SHELX-2018 [40] package was used for structure solution and refinement. The final structure solution was checked with PLATON [41]. The structure was solved by Direct Methods and refinement using least-square methods on F2 with anisotropic displacement parameters for the non-H atoms. All C-bound H atoms were set to idealized geometry and refined with  $U_{iso}(H) = 1.2 U_{eq}(C)$ , C–H(aromatic) =  $0.94 \text{ \AA}$ , and C–H(methylene) =  $0.98 \text{ \AA}$  using a riding model. The H atoms of the water molecules were located in a difference-Fourier map and the isotropically displacement parameters were set to  $U_{iso}(H) = 1.5 U_{eq}(O)$ . Some water molecules were refined with O–H distances restrained to  $0.85 \text{ \AA}$ . Details of the restraints can be found in the embedded INS-file of the CIF-file. The main refinement parameters of the single-crystal determination are listed in Table 1. Figures were prepared with DIAMOND [42] and POV-RAY [43]. Further details of the crystal structure investigation for the coordination compound may be obtained free of charge from the Cambridge Crystallographic Data Centre (<https://www.ccdc.cam.ac.uk/structures/>) on quoting the deposition number CCDC 2062505.

#### 3.3. Powder X-ray Diffraction (PXRD)

X-ray diffraction patterns were measured at room temperature using a STOE STADI P X-ray powder diffractometer with a germanium monochromated Cu-K $\alpha$  radiation ( $\lambda = 1.54056 \text{ \AA}$ ). Standard measurements were done with a generator voltage of 40 kV and a current of 30 mA. Data collection was carried out in Debye–Scherrer geometry and with a position-sensitive detector over an angular range of 3 to  $91^\circ$  as a 2 theta scan type with a step size of  $0.01^\circ$  and a step width of  $0.7^\circ$ . The measuring time of each step of 50 s leads to a total measuring time of approximately 2 h for one range. The total numbers of eight ranges were measured in 16 h. After finishing the data collection, the ranges were added to lower the background noise. This procedure also helped to observe possible changes of the sample during the measurements. Data collection and analysis was performed with the Stoe WINX<sup>POW</sup> software. The JANA2006 program package [39] was used for the Le Bail and Rietveld refinement procedure.

#### 3.4. X-ray Excited Optical Luminescence (XEOL) and Time-Resolved Spectroscopy

Photoluminescence and X-ray excited optical luminescence lifetime spectra were recorded with a fluorescence lifetime spectroscopy system based on a 2D-photon counting streak camera system. The table top system offers three different excitation sources. It includes a pulsed diode laser (Hamamatsu Picosecond Light Pulser) with an excitation wavelength of 444 nm (205 mW, 58 ps pulse width), a pulsed UV-led (Edinburgh Instru-

ments, UK—EPLD 250) with an excitation wavelength of 250 nm (0.4  $\mu$ W, 900 ps pulse width) and a pulsable X-ray tube (Hamamatsu, Japan, N 5084, appr. 80 ps pulse width) with an estimated photon energy of appr. 13–14 keV for high energy excitation of scintillation materials. The measurements were carried out by using a standard generator voltage of 40 kV. The current depends on the chosen time windows and its related pulse repetition rate. Under the chosen conditions of the present experiments a maximum current of 1.1  $\mu$ A is observed. The light collection part of the system consists of a spectrograph (Princeton Instruments, Princeton, NJ, USA—SpectraPro 2150i) with a spectral range of 200–850 nm and two gratings (50 g/mm, blaze 600 nm; 150 g/m, blaze 300 nm) connected to a streak camera (Hamamatsu Streakscope C10627-01). The streak image produced by the streak camera is read out by a fast CCD camera (Hamamatsu C9300-508) and yields in time-resolved fluorescence spectra. From the full time-resolved spectra the wavelength selectable decay times can be determined up to 20 ps. The delay generator (Stanford Research DG 645) synchronizes start pulses of light sources and the streak camera. The Hamamatsu HPD-TA software package was used for system control, data collection and data analysis including decay time fitting. Further set-up details and carried out performance tests of the lifetime spectroscopy system could be found in the literature [6,7].

#### 3.4.1. Sample Preparation for Photoluminescence and Scintillation Measurements

The crystals of the coordination compound were dried for approximately three hours on a filter paper under ambient air conditions and room temperature and grinded in an agate mortar to a very fine powder. The obtained crystalline powder was pressed into a pellet under 10-t pressure and placed in a sample holder (Supplementary Information Figure S6). All luminescence studies were performed using the same powder pellet.

## 4. Conclusions

In summary, the reaction of  $N,N'$ -(1,4-phenylenedicarbonyl)diglycine, 2,2'-bipyridine and cadmium(II) nitrate in alkaline solutions leads to a crystalline scintillating one-dimensional coordination polymer. The X-ray crystallography studies revealed 1D zigzag chains which are linked through a multiplicity of noncovalent interactions of classical and non-classical hydrogen bonding,  $\pi$ - $\pi$  stacking of the electron deficiency aromatic ligands, as well as N-H $\cdots$  $\pi$  and lone-pair- $\pi$  interactions. The metal-organic coordination polymer exhibits a significant fast scintillation under X-ray excitation (photon energy  $\sim$  13–14 keV) with a decay time of 270 ps in the spectral range of 300 to 430 nm with an emission maximum at 363 nm. Moreover, the material shows fluorescence under UV light ( $\lambda_{\text{ex}}$  = 250 nm) and laser ( $\lambda_{\text{ex}}$  = 444 nm) excitation. Due to the fast emission under X-ray excitation, it is conceivable that the Cd(II) coordination polymer can be used for imaging applications such as PET systems. Compared with other common inorganic and organic scintillators measured with the used fluorescence lifetime spectroscopy system, the novel coordination polymer shows a relatively low light yield, which must be increased for use in imaging systems. As a consequence, future work will focus on the behavior under gamma-ray excitation and on the growth of larger single-crystals which are expected to result in a higher light output under the same measuring conditions. The synthesis of further scintillation materials based on the  $N,N'$ -(1,4-phenylenedicarbonyl)diglycinate ligand and metals with high Z are of equal importance.

**Supplementary Materials:** The following are available online at <https://www.mdpi.com/article/10.3390/solids2040023/s1>, Table S1: Hydrogen-bond geometry; Figure S1: The percentage contributions of the different close contacts to the total HS of (a) the  $N,N'$ -(1,4-phenylenedicarbonyl)diglycinate ligand L1 as well as (b) the  $N,N'$ -(1,4-phenylenedicarbonyl)diglycinate ligand L2 and (c) 2,2'-bipyridine; Figure S2: Spectrum of X-ray (photon energy  $\sim$  13–14 keV,  $\sim$ 80 ps pulse width) excited luminescence of the Cd(II) coordination polymer; Figure S3: Time-resolved streak image of UV-light ( $\lambda_{\text{ex}}$  = 250 nm, 900 ps pulse width, 0.4 mW) induced fluorescence of the Cd(II) coordination polymer and an accumulation time of 180 min at a repetition rate of 10 MHz (X-axis: wavelength; Y-axis: time); Figure S4: Spectrum of UV-light ( $\lambda_{\text{ex}}$  = 250 nm, 900 ps pulse width, 0.4 mW) induced fluorescence of

the Cd(II) coordination polymer; Figure S5: Spectrum of laser ( $\lambda_{\text{ex}} = 444$  nm, 205 mW, 58 ps pulse width) induced fluorescence of the Cd(II) coordination polymer; Figure S6: Sample holder and pellet of the Cd(II) coordination compound for photoluminescence and scintillation measurements; The CIF and the checkCIF output files are included in the Supplementary Materials.

**Acknowledgments:** The author is very indebted to A. Adam and M. Gjikaj for their support and helpful suggestions.

**Conflicts of Interest:** The authors declare no conflict of interest.

**Sample Availability:** Samples of the compounds are available from the author.

## References

1. Röntgen, W.C. On a new kind of rays. *Science* **1896**, *3*, 227–231. [[CrossRef](#)]
2. Edison, T. Communication to Lord Kelvin. *Nature* **1896**, *53*, 470–474. [[CrossRef](#)]
3. Boyes, W. *Instrumentation Reference Book*, 4th ed.; Butterworth-Heinemann/Elsevier: Amsterdam, Boston, 2010; ISBN 978-0-7506-8308-1.
4. Fabjan, C.W.; Schopper, H. *Particle Physics Reference Library: Volume 2: Detectors for Particles and Radiation*, 1st ed.; Springer International Publishing: Cham, Switzerland, 2020; ISBN 978-3-030-35318-6.
5. Lecoq, P. Development of new scintillators for medical applications. *Nucl. Instrum. Methods Phys. Res. Sect. A Accel. Spectrometers Detect. Assoc. Equip.* **2016**, *809*, 130–139. [[CrossRef](#)]
6. Pook, N.-P.; Fruhner, C.-J.; Franzl, T.; Denzer, U.; Adam, A. Instrumentation for X-ray excited and laser induced fluorescence lifetime spectroscopy using two-dimensional photon counting. *IEEE Trans. Nucl. Sci.* **2012**, *59*, 2319–2323. [[CrossRef](#)]
7. Pook, N.-P.; Fruhner, C.-J.; Franzl, T.; Denzer, U.; Adam, A. Further performance tests of a picosecond X-ray and laser induced streak camera system with fast scintillation materials. *Radiat. Meas.* **2013**, *56*, 281–284. [[CrossRef](#)]
8. Nikl, M.; Yoshikawa, A. Recent R&D trends in inorganic single-crystal scintillator materials for radiation detection. *Adv. Opt. Mater.* **2015**, *3*, 463–481. [[CrossRef](#)]
9. Yamada, T.; Otsubo, K.; Makiura, R.; Kitagawa, H. Designer coordination polymers: Dimensional crossover architectures and proton conduction. *Chem. Soc. Rev.* **2013**, *42*, 6655–6669. [[CrossRef](#)] [[PubMed](#)]
10. Cook, T.R.; Zheng, Y.-R.; Stang, P.J. Metal-organic frameworks and self-assembled supramolecular coordination complexes: Comparing and contrasting the design, synthesis, and functionality of metal-organic materials. *Chem. Rev.* **2013**, *113*, 734–777. [[CrossRef](#)]
11. Perry, J.J.; Perman, J.A.; Zaworotko, M.J. Design and synthesis of metal-organic frameworks using metal-organic polyhedra as supermolecular building blocks. *Chem. Soc. Rev.* **2009**, *38*, 1400–1417. [[CrossRef](#)] [[PubMed](#)]
12. Kitagawa, S.; Kitaura, R.; Noro, S. Functional porous coordination polymers. *Angew. Chem. Int. Ed. Engl.* **2004**, *43*, 2334–2375. [[CrossRef](#)]
13. Peedikakkal, A.M.P.; Adarsh, N.N. Porous coordination polymers. In *Functional Polymers*; Jafar Mazumder, M.A., Sheardown, H., Al-Ahmed, A., Eds.; Springer International Publishing: Cham, Switzerland, 2019; pp. 181–223. ISBN 978-3-319-95986-3.
14. Heine, J.; Müller-Buschbaum, K. Engineering metal-based luminescence in coordination polymers and metal-organic frameworks. *Chem. Soc. Rev.* **2013**, *42*, 9232–9242. [[CrossRef](#)]
15. Allendorf, M.D.; Bauer, C.A.; Bhakta, R.K.; Houk, R.J.T. Luminescent metal-organic frameworks. *Chem. Soc. Rev.* **2009**, *38*, 1330–1352. [[CrossRef](#)] [[PubMed](#)]
16. Allendorf, M.D.; Foster, M.E.; Léonard, F.; Stavila, V.; Feng, P.L.; Doty, F.P.; Leong, K.; Ma, E.Y.; Johnston, S.R.; Talin, A.A. Guest-induced emergent properties in metal-organic frameworks. *J. Phys. Chem. Lett.* **2015**, *6*, 1182–1195. [[CrossRef](#)]
17. Doty, F.P.; Bauer, C.A.; Skulan, A.J.; Grant, P.G.; Allendorf, M.D. Scintillating metal-organic frameworks: A new class of radiation detection materials. *Adv. Mater.* **2009**, *21*, 95–101. [[CrossRef](#)]
18. Lu, J.; Wang, S.-H.; Li, Y.; Wang, W.-F.; Sun, C.; Li, P.-X.; Zheng, F.-K.; Guo, G.-C. Heat-resistant Pb(ii)-based X-ray scintillating metal-organic frameworks for sensitive dosage detection via an aggregation-induced luminescent chromophore. *Dalton Trans.* **2020**, *49*, 7309–7314. [[CrossRef](#)]
19. Wang, X.; Wang, Y.; Wang, Y.; Liu, H.; Zhang, Y.; Liu, W.; Wang, X.; Wang, S. Color-tunable X-ray scintillation based on a series of isotypic lanthanide-organic frameworks. *Chem. Commun.* **2019**, *56*, 233–236. [[CrossRef](#)] [[PubMed](#)]
20. Lu, J.; Xin, X.-H.; Lin, Y.-J.; Wang, S.-H.; Xu, J.-G.; Zheng, F.-K.; Guo, G.-C. Efficient X-ray scintillating lead(ii)-based MOFs derived from rigid luminescent naphthalene motifs. *Dalton Trans.* **2019**, *48*, 1722–1731. [[CrossRef](#)] [[PubMed](#)]
21. Wang, C.; Volotskova, O.; Lu, K.; Ahmad, M.; Sun, C.; Xing, L.; Lin, W. Synergistic assembly of heavy metal clusters and luminescent organic bridging ligands in metal-organic frameworks for highly efficient X-ray scintillation. *J. Am. Chem. Soc.* **2014**, *136*, 6171–6174. [[CrossRef](#)]
22. Janiak, C. A critical account on  $\pi$ - $\pi$  stacking in metal complexes with aromatic nitrogen-containing ligands. *J. Chem. Soc. Dalton Trans.* **2000**, *21*, 3885–3896. [[CrossRef](#)]
23. Constable, E.C.; Housecroft, C.E. The Early years of 2,2'-Bipyridine-A ligand in its own lifetime. *Molecules* **2019**, *24*, 3951. [[CrossRef](#)]

24. Pook, N.-P. Supramolecular architecture in a Ni(II) complex with a weakly bonded N,N'-(1,4-phenylenedi-carbonyl)diglycinate counter-anion: Crystal structure investigation and hirshfeld surface analysis. *Crystals* **2019**, *9*, 615. [CrossRef]
25. Pook, N.-P.; Adam, A.; Gjikaj, M. Crystal structure and Hirshfeld surface analysis of ( $\mu$ -2-[4-(carboxyl-atomethyl)carbamo-ylbenz-amido]-acetato- $\kappa$ 2O:O')bis-bis-(1,10-phenanthroline- $\kappa$ 2N,N')copper(II) dinitrate N,N'-(1,4-phenyl-enedicarbon-yl)diglycine monosolvate octa-hydrate. *Acta Crystallogr. E Crystallogr. Commun.* **2019**, *75*, 667–674. [CrossRef] [PubMed]
26. Pook, N.-P.; Gjikaj, M.; Adam, A. Bisbis-(2,2'-bi-pyridine- $\kappa$ (2) N,N')(carbon-ato- $\kappa$ (2) O,O')cobalt(III) 2-[4-(carboxyl-atomethyl)carbamo-ylbenz-amido]-acetate hexa-hydrate. *Acta Crystallogr. Sect. E Struct. Rep. Online* **2014**, *70*, m160–m161. [CrossRef]
27. Pook, N.-P.; Hentrich, P.; Gjikaj, M. Crystal structure of bis-tris-(1,10-phenanthroline- $\kappa$ (2) N,N')cobalt(II) tetra-nitrate N,N'-(1,4-phenyl-enedicarbon-yl)diglycine solvate octa-hydrate. *Acta Crystallogr. E Crystallogr. Commun.* **2015**, *71*, 910–914. [CrossRef] [PubMed]
28. Cherni, S.; Abdessatar, C.; Driss, A. Crystal structure of bicapped trigonal-antiprismatic coordinated Cd(II) complex [Cd(C<sub>10</sub>H<sub>8</sub>N<sub>2</sub>)(NO<sub>3</sub>)<sub>2</sub>(H<sub>2</sub>O)]. *X-Ray Struct. Anal. Online* **2012**, *28*, 13–14. [CrossRef]
29. Pan, L.; Huang, X.; Li, J. Assembly of new coordination frameworks in a pH-controlled medium: Syntheses, structures, and properties of 3 $\infty$ [Cd(Hpdc)(H<sub>2</sub>O)] and 3 $\infty$ [Cd<sub>3</sub>(pdc)<sub>2</sub>(H<sub>2</sub>O)<sub>2</sub>]. *J. Solid State Chem.* **2000**, *152*, 236–246. [CrossRef]
30. He, Y.C.; Xiao, L.Y.; Yuan, Z.H.; Zhang, J.; Wang, Y.; Xu, N. Two coordination polymers constructed by 5-(4-carboxyphenoxy)methylbenzene-1,3-dicarboxylic acid and 2,2'-bipyridine: Syntheses, structures and luminescence properties. *Acta Crystallogr. C Struct. Chem.* **2019**, *75*, 1562–1568. [CrossRef]
31. Zhou, D.-M.; Zhao, X.-L.; Liu, F.-Y.; Kou, J.-F. Synthesis and crystal structures of two coordination polymers and a binuclear cadmium(II) complex containing 3- and 4-aminobenzoate ligands. *Acta Crystallogr. C Struct. Chem.* **2015**, *71*, 673–678. [CrossRef]
32. Granifo, J.; Suarez, S.; Baggio, R. Structure of a dinuclear cadmium complex with 2,2'-bi-pyridine, monodentate nitrate and 3-carb-oxy-6-methyl-pyridine-2-carboxyl-ate ligands: Intra-molecular carbon-yl(lone pair)  $\cdots$   $\pi$ (ring) and nitrate( $\pi$ )  $\cdots$   $\pi$ (ring) inter-actions. *Acta Crystallogr. E Crystallogr. Commun.* **2015**, *71*, 890–894. [CrossRef] [PubMed]
33. Meyer, E.A.; Castellano, R.K.; Diederich, F. Interactions with aromatic rings in chemical and biological recognition. *Angew. Chem. Int. Ed. Engl.* **2003**, *42*, 1210–1250. [CrossRef]
34. Imai, Y.N.; Inoue, Y.; Nakanishi, I.; Kitaura, K. Amide- $\pi$  interactions between formamide and benzene. *J. Comput. Chem.* **2009**, *30*, 2267–2276. [CrossRef] [PubMed]
35. Jain, A.; Ramanathan, V.; Sankaramakrishnan, R. Lone pair  $\cdots$   $\pi$  interactions between water oxygens and aromatic residues: Quantum chemical studies based on high-resolution protein structures and model compounds. *Protein Sci.* **2009**, *18*, 595–605. [CrossRef]
36. Jia, C.; Miao, H.; Hay, B.P. Crystal structure evidence for the directionality of lone pair– $\pi$  interactions: Fact or fiction? *Cryst. Growth Des.* **2019**, *19*, 6806–6821. [CrossRef]
37. Spackman, P.R.; Turner, M.J.; McKinnon, J.J.; Wolff, S.K.; Grimwood, D.J.; Jayatilaka, D.; Spackman, M.A. CrystalExplorer: A program for Hirshfeld surface analysis, visualization and quantitative analysis of molecular crystals. *J. Appl. Crystallogr.* **2021**, *54*, 1006–1011. [CrossRef]
38. Rezende, M.V.D.S.; Montes, P.J.R.; Andrade, A.B.; Macedo, Z.S.; Valerio, M.E.G. Mechanism of X-ray excited optical luminescence (XEOL) in europium doped BaAl<sub>2</sub>O<sub>4</sub> phosphor. *Phys. Chem. Chem. Phys.* **2016**, *18*, 17646–17654. [CrossRef] [PubMed]
39. Petříček, V.; Dušek, M.; Palatinus, L. Crystallographic computing system JANA2006: General features. *Z. Für Krist. Cryst. Mater.* **2014**, *229*, 345–352. [CrossRef]
40. Sheldrick, G.M. Crystal structure refinement with SHELXL. *Acta Crystallogr. C* **2015**, *71*, 3–8. [CrossRef]
41. Spek, A.L. Structure validation in chemical crystallography. *Acta Crystallogr. D Biol. Crystallogr.* **2009**, *65*, 148–155. [CrossRef]
42. Impact, C. Diamond—Crystal and Molecular Structure Visualization. Crystal Impact-Dr. H. Putz and Dr. K. Brandenburg GbR, Bonn, Germany. Available online: <http://www.crystalimpact.com/diamond> (accessed on 15 September 2021).
43. Persistence of Vision Raytracer (Version 3.6) [Computer Software]. Persistence of Vision Pty. Ltd. 2004. Available online: <http://www.povray.org/download/> (accessed on 15 September 2021).